Materials Research. 2019; 22(suppl 1): e20190189
DOI: http://dx.doi.org/10.1590/1980-5373-MR-2019-0189

ToF-SIMS Characterization of Nanostructured ZrO_2 Coatings Applied to Near Equiatomic Ni-Ti Alloy

***Natalia Isabel de Azevedo Lopes*[a]*, *Nelson Henrique Jardim Freire*[a], *Pedro Damas Resende*[a], *Jéssica Dornelas Silva*[a], *Leandro de Arruda Santos*[a], *Franck Béclin*[b], *Vicente Tadeu Lopes Buono*[a]**

[a] *Departamento de Engenharia Metalúrgica e de Materiais, Universidade Federal de Minas Gerais (UFMG), Belo Horizonte, MG, Brasil*
[b] *Unité Matériaux et Transformations, UMR CNRS 8207, Université de Lille, 59655 Villeneuve d'Ascq, France*

Received: February 22, 2019; Revised: July 16, 2019; Accepted: November 02, 2019

The ToF-SIMS technique was applied to analyze thin ZrO_2 coatings deposited on the surface of a Ni-Ti alloy. Due to its nanostructured nature, these films are difficult to characterize by conventional techniques. ZrO_2 coatings were deposited on near equiatomic Ni-Ti wires by pulse electrodeposition. Part of the samples was electrolytically polished before the coating process. The coated samples were then analyzed by ToF-SIMS to evaluate the influence of the deposition time and previous surface electropolishing on the structure of the deposited coating. The results indicate that thicker coatings were produced on the electropolished samples, in comparison with the as-received ones. The best uniformity in thickness was achieved when Ni-Ti samples were previously electropolished followed by ZrO_2 electrodeposition for 1200 seconds. Moreover, it was possible to observe by this technique that the inclusions in the Ni-Ti matrix were not entirely covered by the coating.

Keywords: *ToF-SIMS, nickel-titanium, zirconia electrodeposition, nanocoating, biomaterials.*

1. Introduction

Surface phenomena exert a significant influence on the properties of a material, and the understanding of these regions and their interactions with the environment is fundamental. Nevertheless, the study of nanostructured surfaces is particularly difficult and remains a challenge[1,2]. Time-of-Flight Secondary Ion Mass Spectrometry (ToF-SIMS), one of the leading advancement for the SIMS analysis, appears as a promising technique to overcome the challenges involved in the characterization of nanosurfaces. The results of the ToF-SIMS analysis provide a broad characterization of a surface through depth profiles, mass spectra, element mapping, and three-dimensional (3D) imaging in different depth ranges, as well as the detection of contaminants and impurities[1,3,4].

In ToF-SIMS analysis, the surface of the sample is bombarded by a bundle of primary ions, with energies usually ranging from 10 to 30 keV, which collides with the surface atoms resulting in a transfer of energy and particle tearing from the surface of the sample. These particles, typically ions or molecular fragments, are accelerated towards the detector, and the "flight time" is defined as the amount of time spent between primary beam collision to the sample and the captured signal on the detector. In this way, it is possible to identify and quantify elements and molecules with high mass resolution and also to distinguish between isotopes and species with similar nominal molecular weights[3–7]. In addition, the interaction volume generated by the primary ions is of the order of a few nanometers, reaching only the first two atomic monolayers, resulting in better lateral and depth resolutions than other usual surface analysis techniques[3–7].

In this study, the ToF-SIMS technique was applied to the analysis of difficult-to-characterize nanostructured ZrO_2 films deposited on Ni-Ti wires[8]. The coatings were obtained using pulsed cathodic electrodeposition for different times on wires as received and electrolytically polished. Complementary characterization techniques were also applied: scanning electron microscopy (SEM) and field emission scanning electron microscope (FE-SEM) with energy dispersive X-ray spectrometry (EDX), differential scanning calorimetry (DSC), and X-ray diffraction (XRD).

2. Methodology

Ni-Ti wires produced by Confluent Medical Technologies (Fremont, CA, USA) were used in this study. The wires had the nominal diameter of 1 mm and chemical composition of 51.1 ± 0.2 at.% Ni (Ti - balance). Prior to the ZrO_2 electrodeposition, the samples were prepared in two different ways: the first group of samples was ultrasonically cleaned for 15 minutes in acetone and deionized water, and then the ZrO_2 coating was directly applied on the as-received surface. The second group of samples was electropolished between the cleansing and coating steps. The electropolishing was carried out using a 3.5 $mol \cdot L^{-1}$ H_2SO_4 in methanol electrolyte, setting the potential at 7 V, for 240 seconds[9].

Both electropolishing and electrodeposition were performed using a potentiostat/galvanostat Autolab PGSTAT100N (Metrohm Autolab, Utrecht, The Netherlands) and a standard

---

*e-mail: nlopes@ufmg.br

three-electrode cell, comprising a platinum grid, and a Ag|AgCl electrode (3.0 mol L^{-1} KCl), as the counter and reference electrodes, respectively (Figure 1). For the ZrO_2 electrodeposition a solution of 0.05 mol L^{-1} $ZrOCl_2$, 1.0 g L^{-1} polyDADMAC, and 100 g L^{-1} H_2O, in methanol, was used as the electrolyte. A cathodic pulsed current density of 3 mA cm^{-2} ($t_{on} = t_{off} = 0.005$ seconds) was applied for different times, 1200 and 2400 seconds[8].

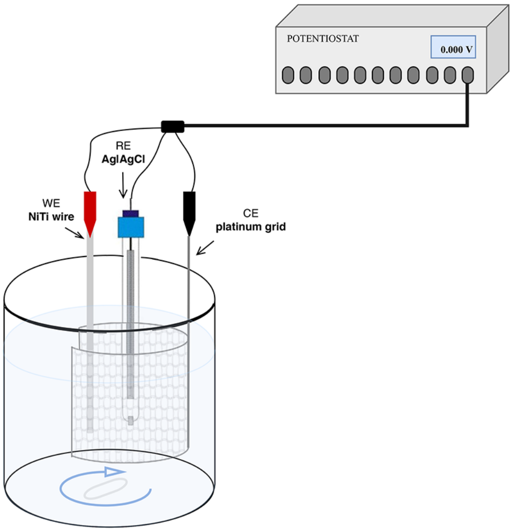

Figure 1. Schematic representation of the experimental setup for the electrodeposition using a three-electrode cell where the NiTi wire is connected as the working electrode (WE), a platinum grid is used as the counter electrode (CE), and an Ag|AgCl electrode is the reference electrode (RE).

DSC measurements were carried out at temperatures ranging from -80°C to 80°C under a controlled cooling/heating rate of 10°C/min using a Q20 calorimeter (TA Instruments, New Castle, USA). Measurements were performed in triplicate, and the phase transformation temperatures were obtained by the tangent interception method, using the software Universal Analysis 2000 from TA Instruments. Phase identification was performed by X-ray diffraction (Empyrean, PANalytical, Almelo, The Netherlands) using a Cu kα radiation source and a scanning rate of $0.02° \cdot s^{-1}$ at the room temperature of 25°C. The obtained diffractograms were compared to reference diffraction patterns available on ICSD database. The surface morphology and semiquantitative chemical composition of the uncoated and coated samples were evaluated by SEM/EDX (Inspect S50, FEI, Hillsboro/ Genesis, EDAX Inc., Mahwah, USA).

The coated samples were prepared by argon ion milling (SEM Mill Model 1060, E. A. Fischione Instruments, Export, USA) to assess the cross-sections of the ZrO_2 coatings. The morphology and the semiquantitative chemical composition were then evaluated by Field Emission Scanning Electron Microscopy – FE-SEM (JSM-7800F LV, JEOL, Tokyo, Japan) equipped with EDX (AZtec, Oxford Instruments, Abingdon, UK).

Finally, samples were analyzed by ToF-SIMS (ToF-SIMS V, IONTOF GmbH, Münster, Germany), equipped with a bismuth liquid metal ion gun. The spectra were taken from each sample in the positive polarity, and no sample preparation was required. The sputtering was performed using an O_2 beam (1 keV) over a 400 µm × 400 µm area. The analyzed area was 75 µm × 75 µm, using Bi_3^+ pulsed primary ion beam (25 keV). The Measurement Explorer IONTOF software was used for data processing. After the ToF-SIMS analyses, the sputtered surfaces of the samples were observed by FE-SEM/EDX.

3. Results and discussion

3.1 Substrate characterization and surface preparation

Figure 2a shows the endothermic and exothermic reactions during a heating/cooling cycle of the as-received Ni-Ti wire obtained by DSC analysis. Upon heating, the sample presented a B19’ (martensite) to B2 (austenite) transformation peak. On cooling, the reverse martensitic transformation (B2 to B19’) occur. The phase transformation temperatures measured by the DSC are listed in Table 1. M_s (martensite start) and M_f (martensite finish) indicate the beginning and end of the martensitic transformation during cooling, whilst A_s (austenite start) and A_f (austenite finish) are the corresponding temperatures for the formation of austenite upon heating. Since the measured A_f temperature is approximately 23°C, the austenite is expected to be the predominant phase of the studied Ni-Ti wire at room temperature (25°C). This is consistent with the observations from XRD (Figure 2b), where only austenite peaks where detected.

Commercially available Ni-Ti wires frequently present scratch marks and other typical surface defects. Many properties of the materials, including corrosion resistance, are closely related to their surface conditions. In bioapplications of Ni-Ti alloys, the corrosion resistance is a constant concern due to the associated release of nickel ions, and its cytotoxic, mutagenic and allergenic activity. Moreover, surface defects and localized corrosion points act as stress concentrators, which can initiate cracking and cause premature failure of biodevices[10–12]. The electrochemical techniques of surface modification, such as polishing and deposition, stand out because they significantly improve the properties of Ni-Ti alloys, and present low cost and high reproducibility[9,10]. Figure 3 illustrates the surface morphologies of the Ni-Ti wire in the as-received state and after electropolishing. The surface of the as-received wire presented a number of pre-existing defects (Figure 3a), such as scratches and inclusions. After electropolishing, the surface scratches were completely removed and a need-like aspect is observed along the entire surface (Figure 3b), which is often associated with a pseudo-martensitic relief structure[13].

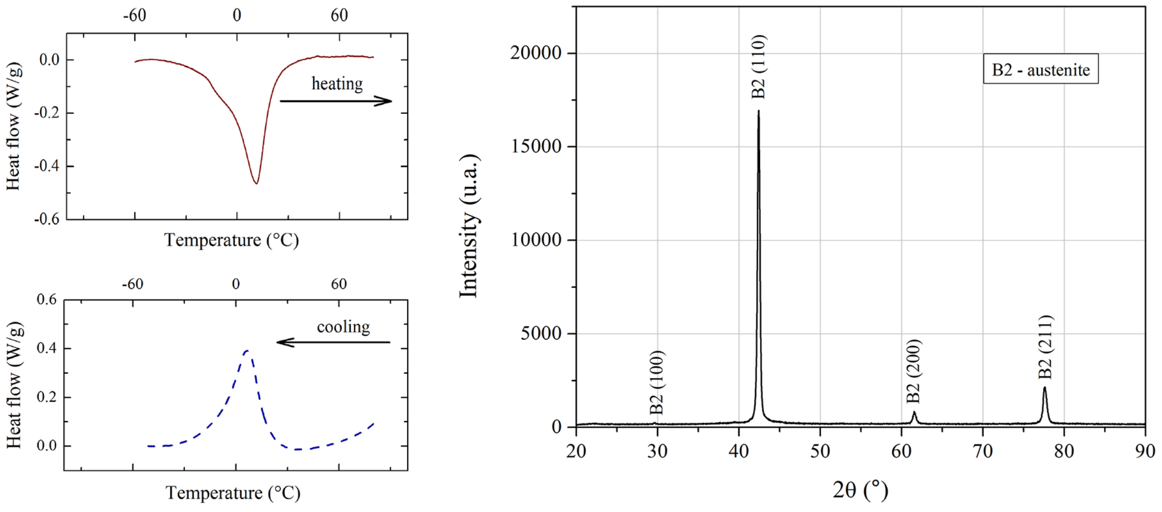

(a) (b)

Figure 2. Initial characterization of the Ni-Ti wire as-received: (a) DSC curve; (b) X-ray diffraction profile.

Table 1. Average transformation temperatures values of the Ni-Ti wires determined by DSC.

Transformation temperatures (°C)			
Martensite start M_s	**Martensite finish M_f**	**Austenite start A_s**	**Austenite finish A_f**
18.7 ± 0.6	-14.1 ± 0.9	-11.1 ± 0.5	23.2 ± 0.8

3.2 Electrodeposited coating and characterization limitations

The cathodic electrodeposition is a widespread process to obtain nanostructured films in various metallic substrates, with important advantages such as thickness control, good uniformity, and purity of the obtained films[14,15]. Previous studies have shown that the application of ZrO_2 coatings improves the corrosion resistance of Ni-Ti alloys, avoid nickel release to the human body, and can potentially reduce its failure in bioapplications[8,16,17]. However, the characterization of ZrO_2 nanocoatings is difficult due to their reduced dimensions. The morphologies of the surfaces after electrodeposition of the ZrO_2 coating for 2400 seconds and the EDX analysis are shown in Figure 4. Even though it has been demonstrated[8] that the electrodeposition of ZrO_2 coating Ni-Ti wires reduces the surface roughness measured by atomic force microscopy (AFM), the assessment of the coating uniformity using SEM is quite challenging. EDX investigations indicated that the zirconium contents on the ZrO_2 coatings were lower than 2 wt.%, making it hard to obtain a reliable evaluation, even when low acceleration potential was used to avoid the substrate interference on the signal. Additionally, no peaks corresponding to ZrO_2 phases where observed by XRD analyses, even using low glancing

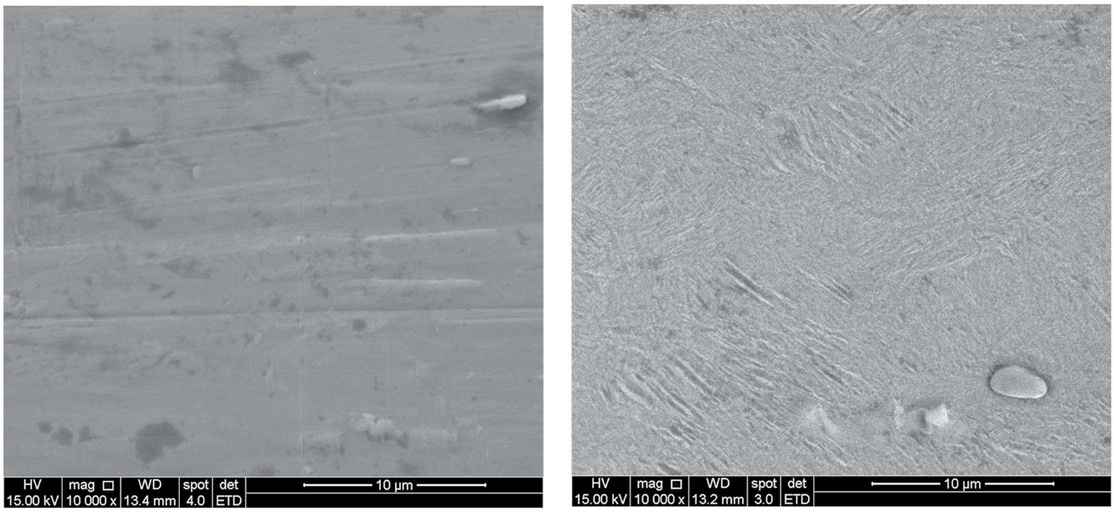

(a) (b)

Figure 3. Surface morphology of the studied Ni-Ti wire: (a) as received; (b) after electropolishing.

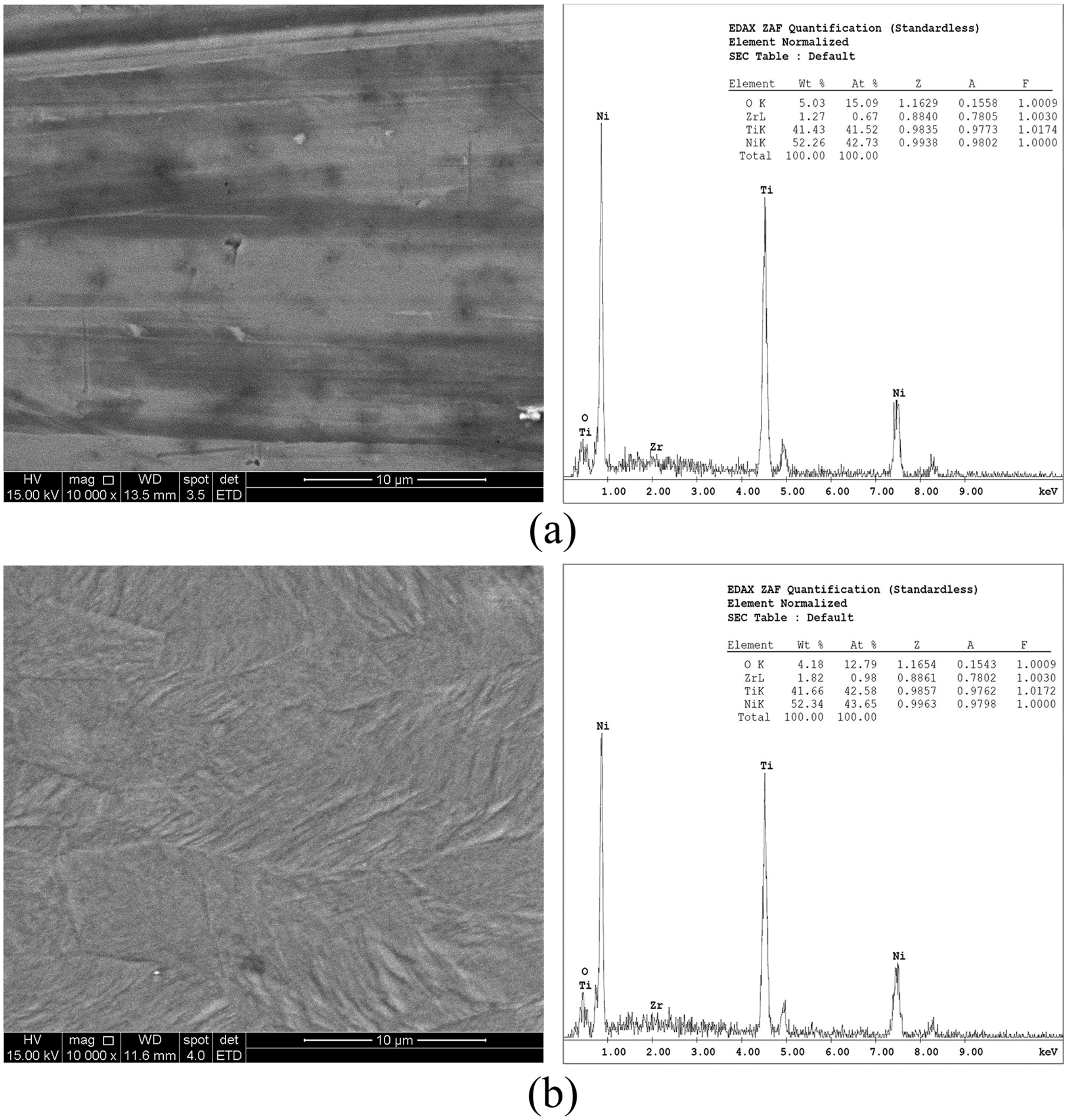

```
EDAX ZAF Quantification (Standardless)
Element Normalized
SEC Table : Default

Element    Wt %    At %       Z        A        F
  O K      5.03   15.09   1.1629   0.1558   1.0009
  ZrL      1.27    0.67   0.8840   0.7805   1.0030
  TiK     41.43   41.52   0.9835   0.9773   1.0174
  NiK     52.26   42.73   0.9938   0.9802   1.0000
 Total   100.00  100.00
```

```
EDAX ZAF Quantification (Standardless)
Element Normalized
SEC Table : Default

Element    Wt %    At %       Z        A        F
  O K      4.18   12.79   1.1654   0.1543   1.0009
  ZrL      1.82    0.98   0.8861   0.7802   1.0030
  TiK     41.66   42.58   0.9857   0.9762   1.0172
  NiK     52.34   43.65   0.9963   0.9798   1.0000
 Total   100.00  100.00
```

Figure 4. SEM and EDX surface images of the Ni-Ti wires coated with ZrO_2: (a) without prior electropolishing; and (b) with prior electropolishing.

angles. This may be explained by the amorphous state of the coating[16,18] or by its low thickness, that hinders its detection.

The cross-section evaluation of the ZrO_2 coating by SEM analysis was not possible when conventional mechanical polishing techniques were used to expose the transverse section of the wire, probably because the coating detached from the specimen during grinding. The use of the argon ion milling technique to expose the coating cross-section produced irregular steps on the specimen surface such as those of the wire electropolished and coated for 2400 seconds shown in Figure 5, most likely due to the differences in sputtering rates of coating and substrate. Although the ZrO_2 coating was visible, the coating thickness could not be precisely measured. However, the line scanning profile provided an estimation of the ZrO_2 coating thickness of approximately 150 nm (Figure 5b).

Hence, the coating morphology and chemical composition could not be precisely characterized, and its thickness could not be assessed.

3.3 ToF-SIMS applied to ZrO_2 characterization

The mass spectrum and secondary ion images obtained by ToF-SIMS provide chemical information for a vast number of applications. However, the experiment is inherently complex and the instrumental parameters have to be carefully selected to obtain the information of interest. For instance, the use of Cs as ion source enhances the yield of electronegative ions, while O_2 enhances the yield of the

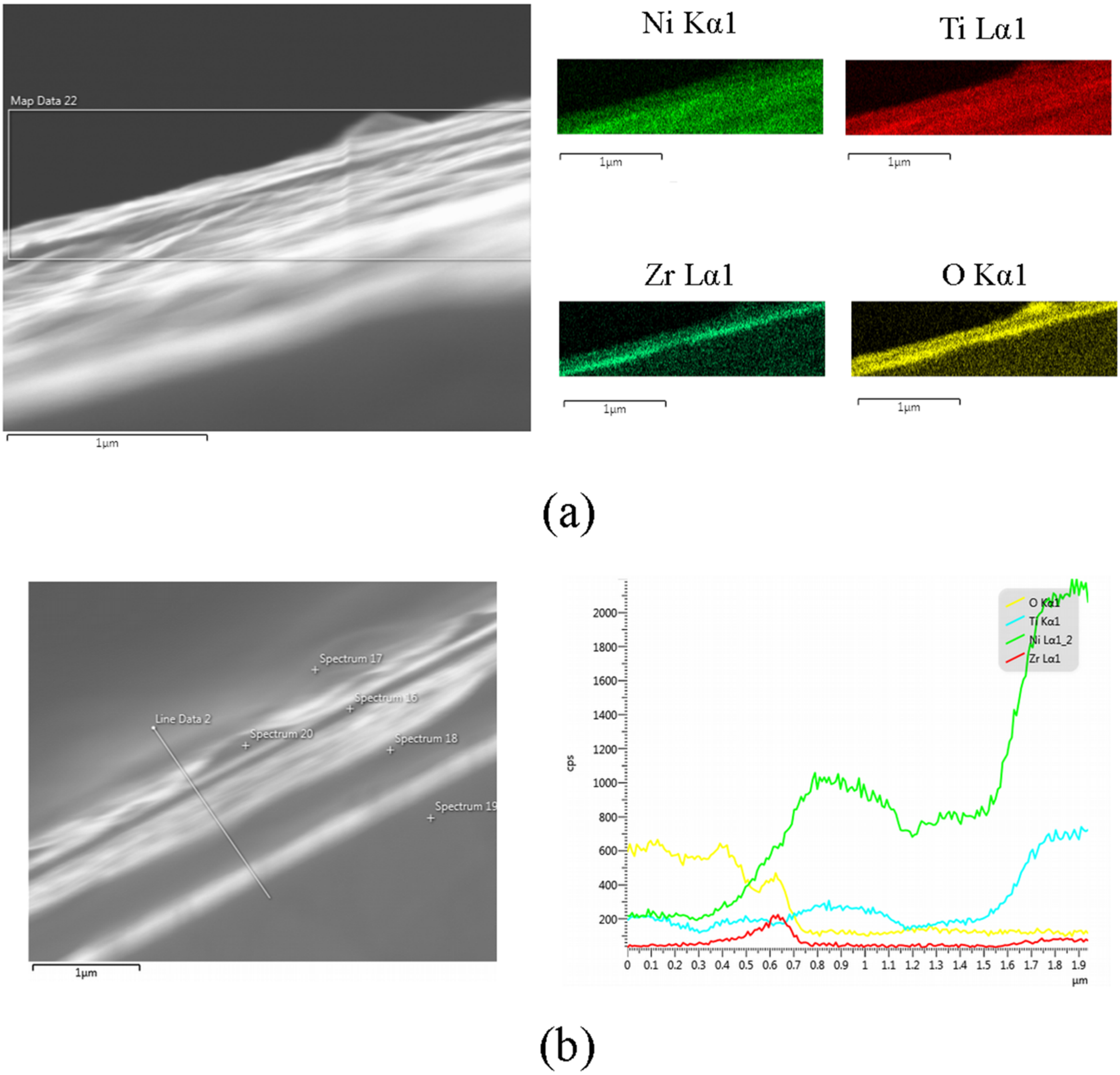

Figure 5. FE-SEM/EDX analysis of the Ni-Ti wire coated with ZrO_2: (a) surface image after ion milling preparation, (b) elemental mapping of the indicated region, (c) line scanning profile.

positive ones. Moreover, the monoatomic Bi^+ ion beam is more appropriate for the detection of inorganic species, whereas polyatomic primary ions (Bi_3^+ and Bi_3^{++}) improve the sensitivity for the detection of high-mass molecular species, such as polymeric additives[3,7,19].

Along with the correct choice of experimental conditions, adequate processing of the acquired data is essential to obtain the target information. The ToF-SIMS spectrum consists of numerous peaks corresponding to fragments of the molecules present at the surface, providing a “fingerprint” that allow the identification of the constituents by comparison to a spectral database. Nevertheless, the analysis of all fragments can be overwhelming and it is not always necessary. According to the aim of the analysis, some characteristic peaks can be selected to identify the compound or to monitor its distribution at the sample volume. In the ToF-SIMS analysis, a full mass spectrum is saved at every volume element, and ion images are collected at each depth during the depth profile measurement[3,4,7,20].

Therefore, the data obtained from ToF-SIMS analyses can be used to generate 3D images of the chemical composition (lateral and depth distribution) of the analyzed samples, as shown in Figure 6. These images provide an enlightening overview of the coating thickness uniformity and as well as the elemental distribution. The thickness of the samples coated without prior electropolishing were estimated to be in a range of 50–60 nm, whereas for the electropolished samples, the estimated thickness is between 80 and 90 nm. When comparing samples with the same surface pretreatment, it can be inferred that longer electrodeposition times result in an increasing of the coating thickness. It can also be observed that for the samples without electropolishing the Ti+ signal is detected in a more external position than the Ni+ signal. This indicates the presence of a TiO_2 layer between the ZrO_2 coating layer and the Ni-Ti substrate. For the samples with prior electropolishing, the differences between the Ni+ and Ti+ signals are less pronounced. This is expected since the electropolishing can dissolve surface irregularities and coarse oxide layers in Ni-Ti alloys, while forming a thin protective layer of TiO_2[9]. The Zr^+ fragments intensity and spatial distribution suggested that the sample of the Ni-Ti wire previously electropolished and with the ZrO_2 coating electrodeposited during 1200 seconds presented the most uniform aspect (Figure 6c). Therefore, this condition was selected to further investigation of the corrosion resistance and further details on these samples structure and properties can be found elsewhere[17]. For the electropolished sample after deposition for 2400 seconds, a considerably decreasing in the thickness uniformity of the coating is observed (Figure 6d). Furthermore, Figure 6c shows an inclusion on the top corner of the 3D model, probably of TiC that does not seem to be covered by the ZrO_2 coating, since only Ti^+ are detected in the outermost layers.

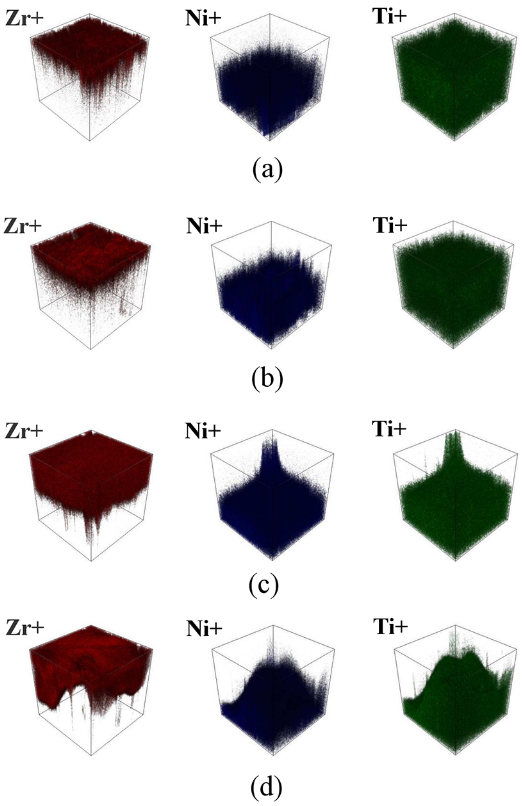

Figure 6. ToF-SIMS 3D models of the Zr+, Ni+ and Ti+ spatial distribution. The edges of the cubes are in the same length scale (200 nm).

Figure 7 shows the ToF-SIMS compositional depth profiling of the coating deposited for 2400 seconds on the surface of the Ni-Ti wires, in which the ions fragments Zr^+, Ni^+ and Ti^+ have been monitored as a function of the sputtering time. These profiles confirm the influence of the electropolishing treatment on the ZrO_2 coating layer thickness. By following the fragments signals, it can be seen that for the sample coated with ZrO_2 without prior electropolishing the Zr^+ signal approaches zero after 300 seconds of analysis time, at the same time as the Ni^+ and Ti^+ signals reach their maximum. Moreover, the Ni^+ signal reaches its maximum significantly after the Ti^+ signal, corroborating the evidence of an intermediate TiO_2 layer between the coating and the substrate. For the sample coated with ZrO_2 with prior electropolishing, the Zr^+ signal approaches zero only after 600 seconds, therefore indicating the higher thickness of the ZrO_2 coating on this sample. Additionally, the ToF-SIMS characterization also allowed to conclude that the polyDADMAC co-deposition did not occur on the reported conditions since none of the typical fragments of the polymer was detected throughout the entire depth profile acquisition, as previously stated.[17].

From the elemental depth profile, several points of interest can be selected and two-dimensional (2D) images of select fragments can be generated for each moment. Figure 8 shows the 2D reconstructed images of the Zr^+, Ni^+ and Ti^+ fragments, of the samples coated with ZrO_2 for 2400 seconds, obtained from different depth ranges of the compositional profile (Figure 7). For the Ni-Ti wire coated without prior electropolishing (Figure 8a), the images were reconstructed integrating the scans obtained from sputtering times from 20 to 40 seconds (corresponding to the ZrO_2 coating), from 120 to 140 seconds (ZrO_2/Ni-Ti interface) and from 350 to 370 seconds (Ni-Ti substrate). In the 2D images corresponding to the ZrO_2 coating, the Zr^+ mapping shows some dark spots, where the Ti^+ and Ni^+ ions were not detected either, indicating a probably surface contamination. Coating defects would have exposed the Ni-Ti substrate and the Ti^+ and Ni^+ ions would have been noticeable. As the sputtering progresses, the Ti^+ and Ni^+ signals become more intense, while the Zr^+ intensity diminishes. Also, most of the dark regions (surface contamination) disappeared. At the end of the analyses, Ti^+ and Ni^+ signals are stronger and the Zr^+ ap proaches zero.

Figure 8b shows 2D reconstructed ion images of the Ni-Ti wire coated after prior electropolishing. The reconstructions were made from scans of sputtering times ranging from 20 to 40 seconds, from 420 to 440 seconds, and of 580 to 600 seconds, for the regions corresponding to the coating, interface, and substrate, respectively. Following the evolution of the Zr^+, Ni^+ and Ti^+ fragments for different sputtering times, similar conclusions can be drawn to those of the sample coated with ZrO_2 for 2400

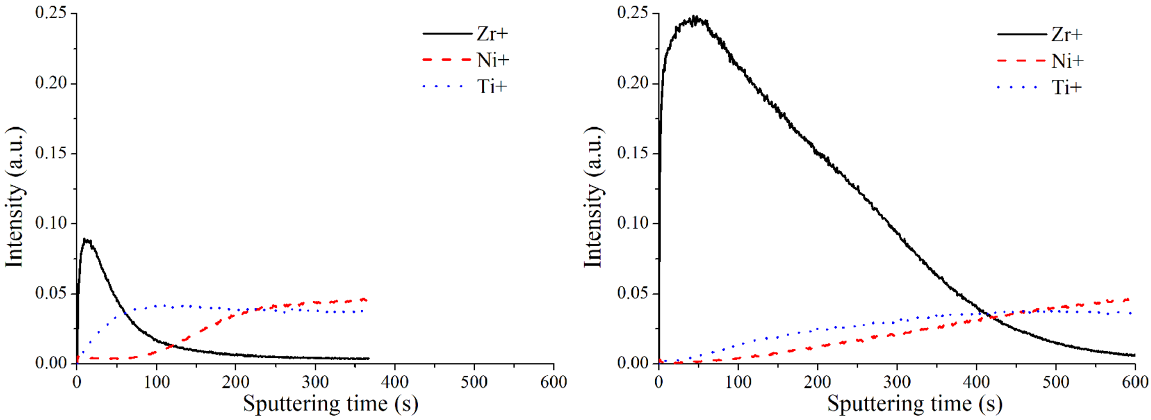

Figure 7. ToF-SIMS compositional depth profiling of Ni-Ti wire coated with ZrO2 (a) without prior electropolishing; and (b) with prior electropolishing.

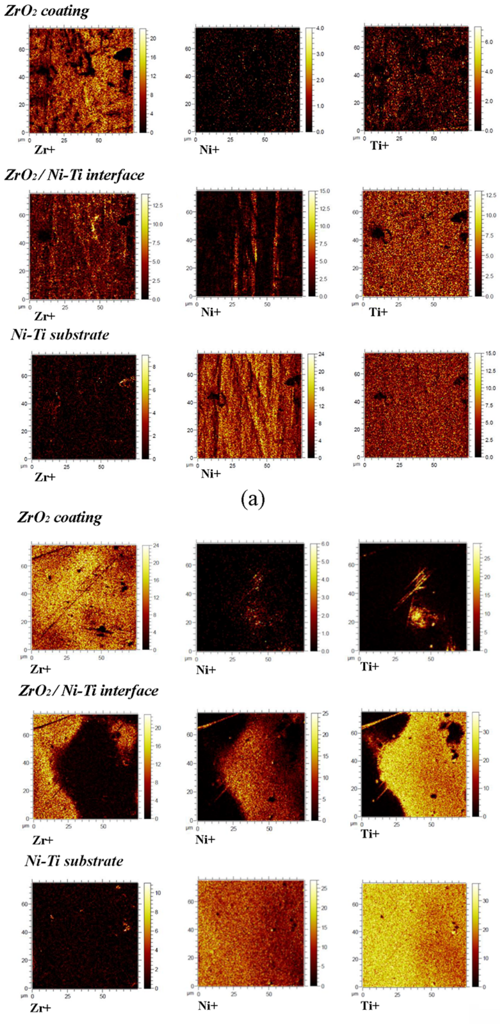

(b)

Figure 8. ToF-SIMS 2D reconstructed ion images of Ni-Ti wire coated with ZrO2 with the electrodeposition time of 2400 seconds: (a) without prior electropolishing; and (b) with prior electropolishing.

seconds without prior electropolishing. Additionally, some scratches on the ZrO_2 coating are visible, and the non-uniformity in terms of coating thickness can be clearly perceived by observing the images reconstructed from 420 to 440 seconds (corresponding to the ZrO_2/Ni-Ti interface). The detection of the thickness irregularity through 2D ion mapping complements the compositional depth profile analysis, shown in Figure 7, providing a more accurate comprehension of the coating structure.

Typical depth profiling artifacts (e.g. variations of sputtering rates of different components and changes on the sputter rates in highly topographic samples) can be corrected to accurately reconstruct the depth profiles[21]. Nevertheless, assuming that the sputter rate through the sample is uniform, the depth calibration can be performed by calculating the sputter rate based on the total sputtering time elapsed to reach a known depth profiles[22]. That is, the measurement of the depth of the final crater can allow the profile depth calibration. However, in our study, the ToF-SIMS crater could not be measured by FE-SEM/EDX (Figure 9) and AFM techniques (data not shown) due to the nanometric scale of the coating.

Furthermore, elemental quantification, to convert intensity to concentration, was not performed in our study. The quantification of chemical elements using ToF-SIMS is not straightforward since the fragment intensity depends not only on its concentration but also on the ion yield that can vary with its surrounding environment. This is called the “matrix effect” which, along with depth calibration complications, makes challenging to convert the ToF-SIMS data from intensity vs. time to concentration vs. depth profile. To overcome this limitation the ToF-SIMS analysis can be combined with many other techniques[3,4,7], which is beyond the scope of this study.

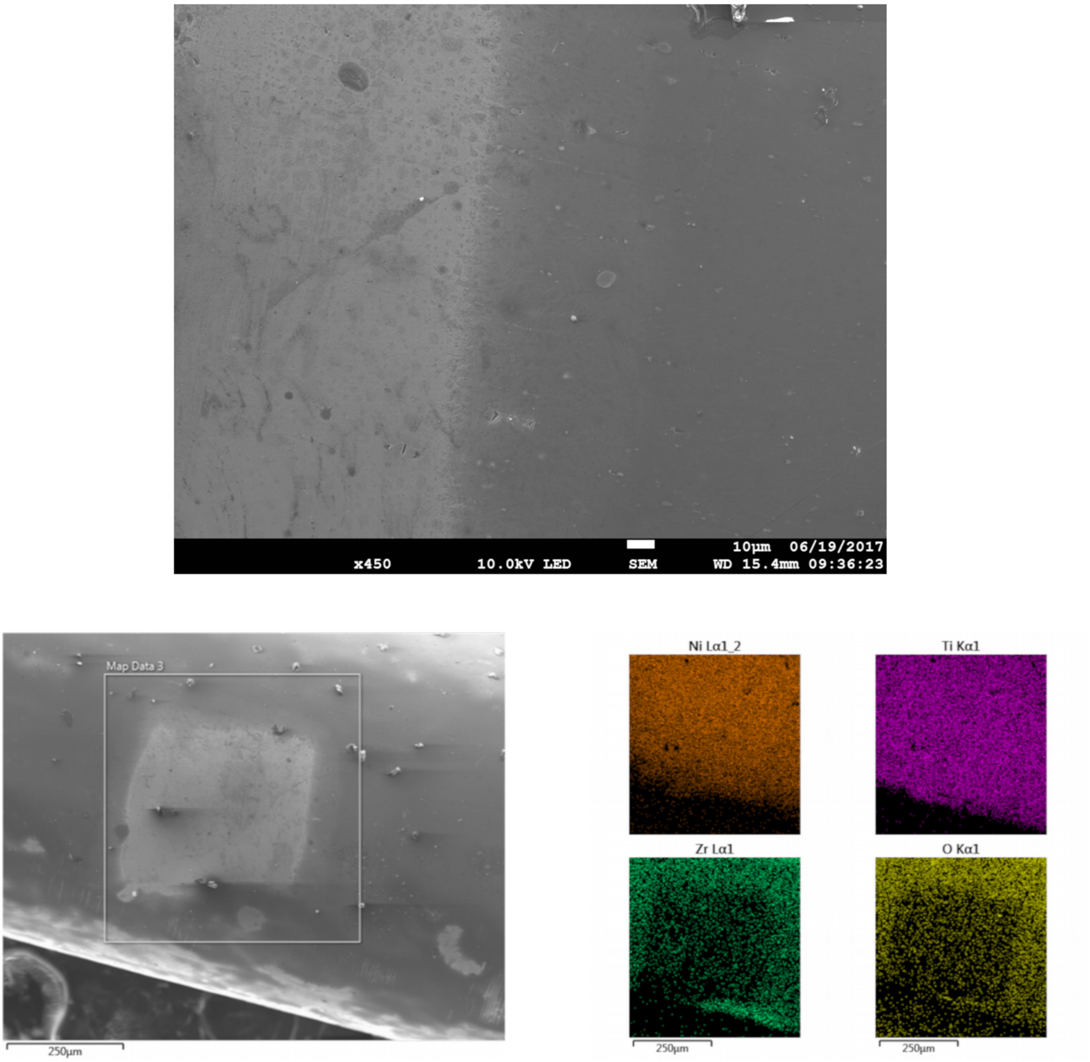

Figure 9. FE-SEM/EDX analysis of the surface of Ni-Ti wire coated with ZrO_2 after ToF-SIMS analysis.

4. Conclusions

Nanometric ZrO_2 coatings obtained by electrodeposition on superelastic Ni-Ti wires were characterized using ToF-SIMS. The results allowed observing the compositional depth profile and spacial distribution of the elements of the deposited coatings. These profiles show that the application of electropolishing as a surface treatment before the ZrO_2 deposition results in thicker coating layers when compared with the coatings deposited straight on the as-received wires. Considering the samples with the same surface preparation, longer electrodeposition times increased the coating thickness. However, for the electropolished wire the thickness uniformity decreased when longer deposition time was used. Also, it has been shown that the inclusions in the matrix are not completely covered by the ZrO_2 coating. Hence, ToF-SIMS technique proved to be a valuable characterization tool for ZrO_2 coatings difficult to study by conventional techniques, and a promising technique for understanding surface and interface phenomena of nanomaterials.

5. Acknowledgements

This study was financed in part by the Conselho Nacional de Desenvolvimento Científico e Tecnológico (CNPq), the Fundação de Amparo à Pesquisa do Estado de Minas Gerais (FAPEMIG), and the Coordenação de Aperfeiçoamento de Pessoal de Nível Superior - Brasil (CAPES) - Finance Code 001. Chevreul Institute (FR 2638), Ministère de l'Enseignement Supérieur et de la Recherche, Région Nord – Pas de Calais, FEDER and the European Commission in the framework of Erasmus Mundus - IBRASIL are acknowledged for supporting and partially funding this work. The authors also gratefully acknowledged Nicolas Nuns (UCCS/Lille University, France) for the ToF-SIMS analyses.

6. References

1. Baer DR, Engelhard MH, Johnson GE, Laskin J, Lai J, Mueller K, et al. Surface characterization of nanomaterials and nanoparticles: Important needs and challenging opportunities. *Journal of Vacuum Science & Technology A*. 2013;31(5):050820.

2. Baer DR, Amonette JE, Engelhard MH, Gaspar DJ, Karakoti AS, Kuchibhatla S, et al. Characterization challenges for nanomaterials. *Surface and Interface Analysis*. 2008;40(3-4):529-337.

3. Sodhi RNS. Time-of-flight secondary ion mass spectrometry (TOF-SIMS): - versatility in chemical and imaging surface analysis. *Analyst*. 2004;129(6):483-487.

4. Belu AM, Graham DJ, Castner DG. Time-of-flight secondary ion mass spectrometry: techniques and applications for the characterization of biomaterial surfaces. *Biomaterials*. 2003;24(21):3635-3653.

5. Stevie FA. *Secondary Ion Mass Spectrometry: Applications for Depth Profiling and Surface Characterization*. New York: Momentum Press; 2015.

6. Fearn S. Characterisation of biological material with ToF-SIMS: a review. *Materials Science and Technology*. 2015;31(2):148-161.

7. Vickerman JC. Prologue ToF-SIMS – An evolving mass spectrometry of materials. In: Vickerman JC, Briggs D, eds. *ToF-SIMS – Surface Analysis by Mass Spectrometry*. 2nd ed. Manchester: SurfaceSpectra; 2013.

8. Lopes NIA, Freire NHJ, Resende PD, Santos LA, Buono VTL. Electrochemical deposition and characterization of ZrO_2 ceramic nanocoatings on superelastic NiTi alloy. *Applied Surface Science*. 2018;450:21-30.

9. Lopes NIA, Silva LAO, Santos LA, Buono VTL. Surface Characterization of NiTi Superelastic and Shape Memory Alloys After Electrolytic Polishing. *Materials Research*. 2017;20(Suppl 2):572-579.

10. Shabalovskaya S, Anderegg J, Van Humbeeck J. Critical overview of Nitinol surfaces and their modifications for medical applications. *Acta Biomaterialia*. 2008;4(3):447-467.

11. Rokicki R, Hryniewicz T, Pulletikurthi C, Rokosz K, Munroe N. Towards a Better Corrosion Resistance and Biocompatibility Improvement of Nitinol Medical Devices. *Journal of Materials Engineering and Performance*. 2015;24(4):1634-1640.

12. Rits J, van Herwaarden JA, Jahrome AK, Krievins D, Moll FL. The Incidence of Arterial Stent Fractures with Exclusion of Coronary, Aortic, and Non-arterial Settings. *European Journal of Vascular and Endovascular Surgery*. 2008;36(3):339-345.

13. Pohl M, Heßing C, Frenzel J. Electrolytic processing of NiTi shape memory alloys. *Materials Science and Engineering: A*. 2004;378(1-2):191-199.

14. Zhitomirsky I. Cathodic electrodeposition of ceramic and organoceramic materials. Fundamental aspects. *Advances in Colloid and Interface Science*. 2002;97(1-3):279-317.

15. Zhitomirsky I, Petric A. Cathodic electrodeposition of polymer films and organoceramic films. *Materials Science and Engineering: B*. 2000;78(2-3):125-130.

16. Giacomelli FC, Giacomelli C, de Oliveira AG, Spinelli A. Effect of electrolytic ZrO_2 coatings on the breakdown potential of NiTi wires used as endovascular implants. *Materials Letters*. 2005;59(7):754-758.

17. Lopes NIA, Freire NHJ, Silva JD, Lins VFC, Legris A, Béclin F, et al. Corrosion resistance and stability of zirconia nanostructured thin film applied to near-equiatomic nickel-titanium alloy.

18. Yen SK, Huang TY. Characterization of the electrolytic ZrO_2 coating on Ti-6A1-4V. *Materials Chemistry and Physics*. 1998;56(3):214-221.

19. Smentkowski VS. Surface analysis of ceramics by time of flight secondary ion mass spectrometry (TOF-SIMS). *American Ceramic Society Bulletin*. 2012;91(1):30-35.

20. Smentkowski VS, Ostrowski SG, Braunstein E, Keenan MR, Ohlhausen JA, Kotula PG. Multivariate Statistical Analysis of Three-Spatial-Dimension TOF-SIMS Raw Data Sets. *Analytical Chemistry*. 2007;79(20):7719-7726.

21. Taylor AJ, Graham DJ, Castner DG. Reconstructing accurate ToF-SIMS depth profiles for organic materials with differential sputter rates. *Analyst*. 2015;140(17):6005-6014.

22. Grehl T, Möllers R, Niehuis E, Rading D. Application of TOF-SIMS for high precision ion implant dosimetry: Possibilities and limitations. *Applied Surface Science*. 2008;255(4):1404-1407.